# Locating Faults by Using Incremental Quantities: Introduction, Application Considerations, and Performance

Bogdan Kasztenny and Greg Smelich
*Schweitzer Engineering Laboratories, Inc.*

Presented at the
52nd Annual Western Protective Relay Conference
Spokane, Washington
October 28–30, 2025

# Locating Faults by Using Incremental Quantities: Introduction, Application Considerations, and Performance

Bogdan Kasztenny and Greg Smelich, *Schweitzer Engineering Laboratories, Inc.*

***Abstract*—This paper presents a multi-ended fault-locating method that works in the time domain, i.e., it uses samples from an arbitrary data window rather than phasors. The method is based on the observation that the change in voltage at the fault location estimated from the local terminal is the same as that estimated from the remote terminal. The method uses the measured instantaneous incremental voltage and instantaneous incremental replica current to calculate the change in voltage at the fault location as a function of the per-unit distance to the fault. The method applies the Least Errors Squared (LES) algorithm with an arbitrary data window to find the value of the distance to the fault that yields the closest match between the two calculated voltage changes. To improve accuracy and avoid faulted-loop selection, the method uses the LES approach to match voltage changes in multiple loops regardless of the fault type. The method works very well for evolving and short-lived faults as well as for resistive faults, including arcing faults. This paper is an expanded version of our original work [1] and explains how to apply the method to cables and hybrid lines, includes an application with data that are not time aligned, and provides an incipient fault example, among other topics.**

## I. Introduction

Accurate and dependable fault locating improves power system operations by shortening the line inspection time, streamlining the repair work, and leading to faster restoration of critical lines.

Traveling-wave-based fault locators (TWFLs) are accurate and dependable. The pace of TWFL installations has increased steadily in the last two decades, and since 2012, TWFLs have been available in line protective relays [2] [3]. However, in rare cases, such as an unfavorable type of line termination or faults with precursors, a TWFL can fail to locate a fault, making an accurate backup fault-locating method necessary.

Ultra-high-speed (UHS) line protective relays that are based on fault transients (incremental quantities and traveling waves) [4] emerged in the last decade. These relays [5] [6] routinely trip in less than 3 ms. When applied with two-cycle breakers, UHS relays often clear line faults in 1.5 power cycles. Such a short fault-clearing time challenges fault locators that are based on phasors. A full-cycle phasor estimator takes about 1.25 cycles to obtain a stable phasor. Just when the phasor becomes stable at 1.25 cycles, the breaker starts to open at 1.5 cycles. As a result, a phasor-based fault locator may have less than 0.25 cycle of stable fault phasor data to work with. Transients present in the voltages and currents during faults extend the phasor estimator settling time. As a result, a phasor-based fault locator may have no accurate data to work with for faults cleared in 1.5 cycles.

Shortening the phasor data window to cope with a shorter fault duration reduces phasor accuracy and is therefore counter-productive in an accuracy-focused application such as fault locating.

Addressing evolving faults is another motivation for this work. During an evolving fault, such as when an AG fault evolves into an ABG fault in a few milliseconds, an extra transition in the currents and voltages occurs between the fault inception and breaker operation. As a result, a full-cycle phasor estimator may never stabilize during an evolving fault.

Incipient cable faults, i.e., faults that last half a power cycle or just a few half cycles before they clear on their own, pose another fault-locating challenge. If a fault lasts only half a cycle (or less), a full-cycle phasor estimator does not reach a stable response at all. Measuring a current phasor by using only half a cycle of fault data is especially challenging because of the decaying dc component in the fault current. This dc component brings significant uncertainty as to the magnitude of the fault current if only half a cycle of data is available.

We seek a multi-ended fault-locating method that is capable of working on a short fault data window despite transients that occur within that window. Another objective is to improve fault-locating dependability and accuracy in low-sampling-rate applications and fault-locating dependability in high-sampling-rate (TW-based) applications.

To achieve these objectives, we developed a method with the following characteristics:

- The method uses moderate sampling rates and can be deployed in a typical line protective relay that samples on the order of a few kilohertz or offline by using waveforms from a typical digital fault recorder.
- The method uses only the positive-sequence line impedance to avoid errors associated with the zero-sequence line impedance.
- The method uses an arbitrary data window size, allowing for windows as short as half a power cycle.
- The method is unaffected by the placement of the data window with respect to the fault inception as long as a significant portion of the data window includes the fault state.
- The method works without faulted-loop selection logic and therefore performs well for evolving faults,

including internal faults at the same location as well as external-to-internal and internal-to-external faults.
- The method works for high-resistance, intermittent, and arcing faults.
- The method works for multiterminal lines by identifying the faulted line section and providing the fault location within that section.
- The method works for hybrid lines comprising overhead line sections and underground cable sections.

This paper derives the new method (Section II) and illustrates it with several examples that use faults recorded in the field (Section III). Section IV discusses the accuracy and important characteristics of the method. Sections V, VI, and VII address applications to multiterminal, cable, and hybrid lines. Section VIII addresses the application of the method with local and remote records that are not time-aligned. Finally, to support the accuracy claims, Section IX shows the performance of the method for over 100 faults recorded in the field.

## II. New Time-Domain Fault-Locating Method

### A. Basic Principle

Consider a power line between the local terminal L and the remote terminal R, as shown in Fig. 1. $Z_1$ is the complex positive-sequence line impedance and m is the per-unit fault location relative to the local terminal.

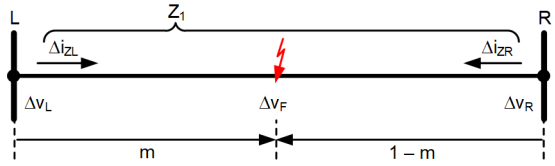


Fig. 1. Power line and associated variables.

Consider instantaneous incremental (Δ) voltages and currents at the local and remote terminals. We obtain the incremental signals by subtracting one- or two-cycle-old values [4]. The subscript Z in $\Delta i_Z$ denotes a replica current, i.e., the current obtained by using a unity impedance that mimics the positive-sequence line impedance ($R_1$ is the line resistance and $L_1$ is the line inductance) [4]:

$$\Delta i_Z = \frac{R_1}{|Z_1|} \cdot \Delta i + \frac{L_1}{|Z_1|} \cdot \frac{d}{dt} \Delta i \qquad (1)$$

We calculate the change in voltage $\Delta v_F$ at a per-unit fault location m by using the local measurements:

$$\Delta v_{FL} = \Delta v_L - m \cdot |Z_1| \cdot \Delta i_{ZL} \qquad (2)$$

Similarly, we calculate the change in voltage $\Delta v_F$ at a per-unit fault location m by using the remote measurements:

$$\Delta v_{FR} = \Delta v_R - (1 - m) \cdot |Z_1| \cdot \Delta i_{ZR} \qquad (3)$$

When calculated for the true fault location $m_0$, the values from (2) and (3) match, as Fig. 2 illustrates.

The incremental voltages and incremental replica currents are instantaneous values (samples). Therefore, the change-in-fault-location-voltage signals (2) and (3) are also instantaneous values, as Fig. 3 illustrates.

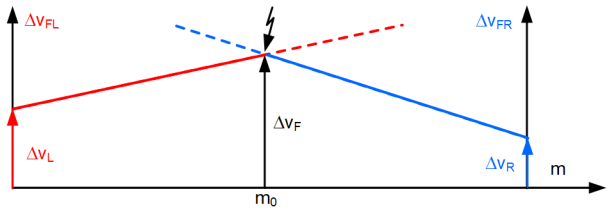


Fig. 2. The local and remote change-in-fault-location-voltage estimates intersect at the true fault location.

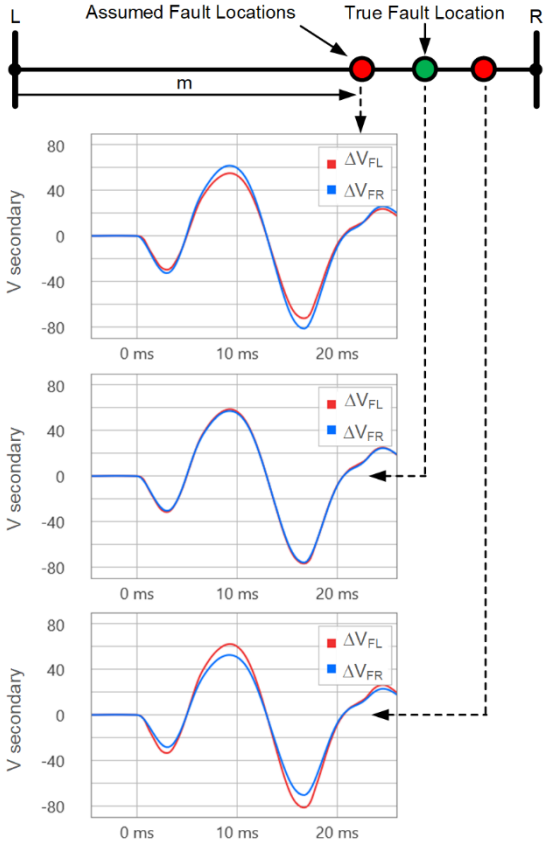


Fig. 3. The change-in-fault-location-voltage signals for the true fault location and two adjacent locations.

The change-in-fault-location-voltage signals develop from zero and reflect the change in voltage from pre-fault to fault values, including transients. The estimate from the local terminal (2) and the remote terminal (3) match for the true fault location, irrespective of the transients. It is, however, beneficial to pass signals (2) and (3) through a low-pass filter to remove signal components that do not depend on the fault location, such as oscillations related to the line capacitance. For example, relays [5] and [6] use second-order filters that attenuate their input signals by –20 dB at 0.4 kHz.

### B. LES Calculations

We use the Least Errors Squared (LES) algorithm to calculate the actual fault location $m_0$ by minimizing the difference between (2) and (3) over a time window $T_W$:

$$\sum_{Tw} (\Delta v_{FL} - \Delta v_{FR})^2 \rightarrow \text{Minimum} \qquad (4)$$

We insert (2) and (3) into (4) and solve for $m_0$ as follows:

$$m_0 = \frac{S_N}{S_D} \tag{5}$$

where the numerator and denominator sums are:

$$S_N = \sum_{T_W} \left( \frac{\Delta v_L - \Delta v_R}{|Z_1|} + \Delta i_{ZR} \right) \cdot (\Delta i_{ZL} + \Delta i_{ZR}) \tag{6}$$

$$S_D = \sum_{T_W} (\Delta i_{ZL} + \Delta i_{ZR})^2 \tag{7}$$

Equations (5), (6), and (7) define our *basic* fault-locating method. These equations are very simple and involve sums over a time window $T_W$ of expressions that combine samples of the local and remote incremental voltages and incremental replica currents.

### C. Loop Quantities

The traditional approach to impedance-based fault locating requires using the voltage and current of the faulted loop. For example, fault locators use the AG loop for A-phase-to-ground faults and the AB loop for A-phase-to-B-phase faults. Our method can be applied in this traditional way by using the instantaneous loop voltages and currents (see [4] for details on forming fault loop voltages and currents in the time domain).

However, our method does not require faulted-loop selection logic and can be applied by using only the phase-to-phase loops. The phase-to-phase voltages at the fault location change for both phase-to-ground and phase-to-phase faults. For example, during an AG fault, the AG, AB, and CA voltages change significantly. Equations (5), (6), and (7) can be applied to the AG loop, the AB loop, and the CA loop and will yield nearly identical results. Therefore, we can use the phase loops for all fault types, including single-phase-to-ground faults.

Using only phase loops improves accuracy by not having to rely on the zero-sequence line impedance, which is typically less accurate than the positive-sequence line impedance. The zero-sequence line impedance depends on soil resistivity along the line path at the time of the fault. Additionally, mutual coupling with parallel lines, rail tracks, and pipelines affects the zero-sequence voltage and current components.

We avoid faulted-loop selection logic by redefining the LES approach (4) to include the sum of differences between the local and remote change-in-fault-location-voltage estimates in the ΦΦ loops as follows:

$$\sum_{\Phi\Phi=AB}^{CA} \sum_{T_W} (\Delta v_{FL\Phi\Phi} - \Delta v_{FR\Phi\Phi})^2 \rightarrow \text{Minimum} \tag{8}$$

where ΦΦ is the phase-to-phase loop index.

We solve the LES problem formulated as (8) and obtain:

$$S_N = \sum_{\Phi\Phi=AB}^{CA} \sum_{T_W} \left( \frac{\Delta v_{L\Phi\Phi} - \Delta v_{R\Phi\Phi}}{|Z_1|} + \Delta i_{ZR\Phi\Phi} \right) \cdot (\Delta i_{ZL\Phi\Phi} + \Delta i_{ZR\Phi\Phi}) \tag{9}$$

$$S_D = \sum_{\Phi\Phi=AB}^{CA} \sum_{T_W} (\Delta i_{ZL\Phi\Phi} + \Delta i_{ZR\Phi\Phi})^2 \tag{10}$$

Equations (5), (9), and (10) define our *advanced* fault-locating method. These equations are very simple and involve sums – over a time window $T_W$ and over all three phase loops – that combine samples of the local and remote phase-to-phase incremental voltages and phase-to-phase incremental replica currents.

We can further expand our method by remembering that the method matches the change-in-fault-location-voltage signals, and it will continue to work if it matches fractions of these signals. Equations (5), (9), and (10) match the phase-to-phase voltages, which are scaled beta Clarke components [2]. The method can also match the alpha components (phase components minus the zero-sequence or ground component), and by doing so, it would eliminate the impact of the zero-sequence line impedance errors. In theory, an expanded method can use (5), (9), and (10) and sum all six aerial components (three alpha components and three beta components) instead of the three phase-to-phase (beta) components. However, we can prove that the $S_N$ and $S_D$ sums for the three beta components are exactly the same as the sums for the three alpha components. Therefore, our advanced method already brings all the benefits of using both the beta and alpha components.

Note that the denominator (10) is never zero for internal faults because it reflects current that flows through the fault path at the fault location. As a result, the method is numerically robust and stable.

### D. Window Selection

Our method allows for flexible selection of the beginning ($T_D$) and length ($T_W$) of the data window (see Fig. 4).

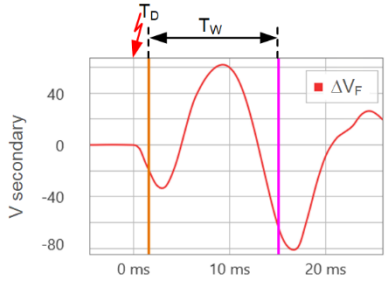


Fig. 4. Data window position and length.

It is beneficial to start the data window a few milliseconds into the fault. This delay allows for purging the data window from transients that do not depend on the fault location. These transients are primarily the high-frequency components in the voltage signals and the step response of the low-pass filters that the fault-locating devices use when acquiring voltages and currents. Also, capacitively coupled voltage transformers (CCVTs) exhibit a low-pass frequency response and smooth the falling edge of the voltage at the fault inception. Avoiding the first one or two milliseconds of data allows us to leave this CCVT artifact out of the input data used by the method. On the other hand, the change-in-fault-location-voltage signal develops from zero and therefore is relatively small in the first few milliseconds after the fault inception. Additionally, the aforementioned transients tend to partially average out. As a result, the initial data do not affect the LES sums much and delaying the data window is beneficial but not strictly required.

The length of the data window ($T_W$) should be shorter than the shortest possible fault duration. In applications with phasor-based relays, consider using $T_W = 2$ cycles. In applications with transient-based UHS relays, consider using $T_W = 1$ cycle. In applications to locate incipient cable faults, consider using $T_W = 0.5$ cycle. Of course, the window length does not need to be a multiple of half a cycle. Also, the window does not need to perfectly envelop the fault interval. The impact of starting the window too early or closing it too late is negligible.

The data window length can be adaptive. For example, the fault-locating logic can close the data window 1 cycle after the relay has issued the trip command. Alternatively, the logic can analyze the current waveform to detect the time of the open-pole condition and close the data window just before the open-pole condition occurs.

## III. Examples of Operation

### *A. Fast-Clearing Fault*

A UHS relay [5] installed on a 345 kV, 109.32 mi line in a 60 Hz system tripped in 2 ms for a BG fault. Owing to the two-cycle breakers, the total fault duration was only 24 ms or 1.44 cycles. Fig. 5 shows the local and remote voltages and currents.

The utility reported the true fault location as 41.91 mi. Our method calculated 42.603 mi (an error of 0.6 percent of the line length). A traditional phasor-based fault-locating method has no accurate data to work with for this fault because just when the full-cycle phasors are about to stabilize, the breaker interrupts the current and initiates a new transient. This absence of a stable phasor is especially pronounced in the voltage signal because the voltage has sizeable transients that last for about half a cycle. When the breaker starts to open, these transients are not flushed from the effective 1.25 cycle data window of the phasor estimator.

Fig. 5 shows the change-in-fault-location-voltage signals (the BC loop) calculated from both terminals of the line according to the new fault-locating method. The two estimates (the red and blue traces in the bottom plot) match very well, as expected for an accurate fault-locating result.

We use this example to demonstrate the sensitivity of the new method to the distance-to-fault value m. Ideally, we want the LES sum to change as much as possible when m changes. Fig. 6 shows the square root of the LES value (8) normalized by dividing it by its highest value for any assumed fault location along the entire line. Note that the value of the square root of the LES sum for the true fault location is only 0.016 pu of the maximum value and the plot is steep, with a single valley clearly pointing to the correct fault location.

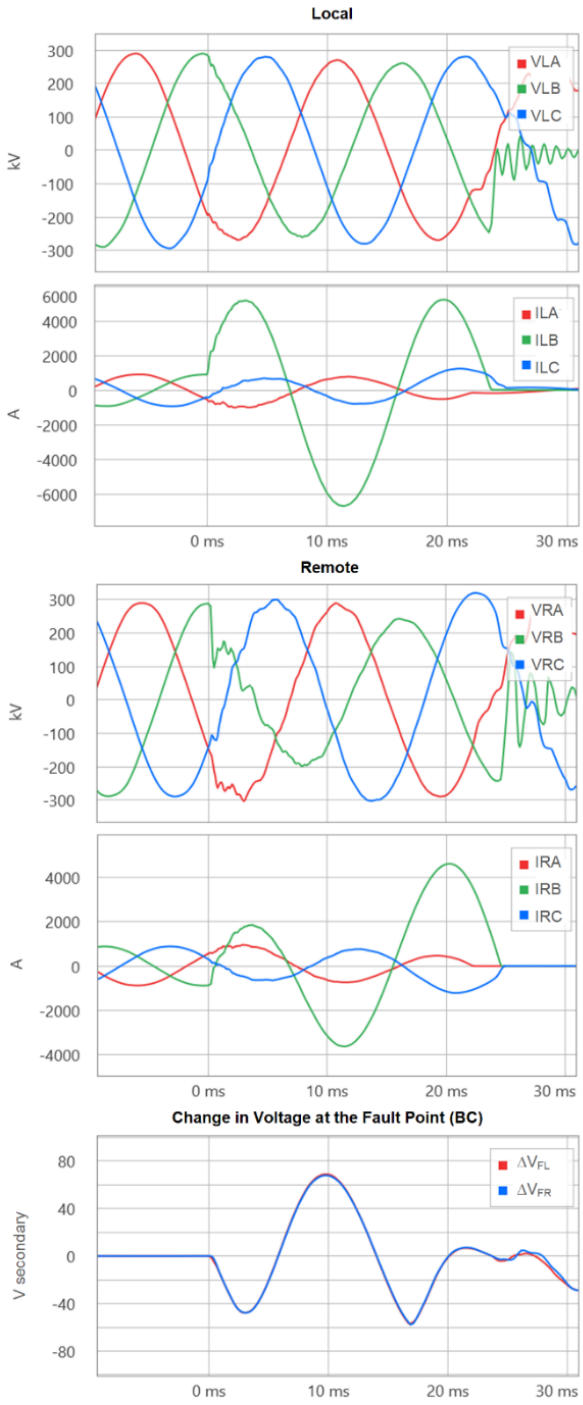


Fig. 5. Fast-clearing fault example.

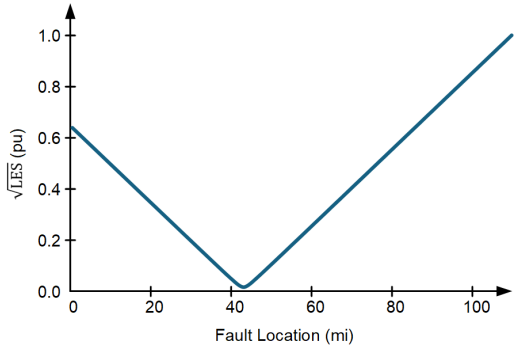


Fig. 6. Sensitivity of the LES sum with respect to the fault location.

We introduce a different measure, the *goodness of fit* value ε, for the purpose of approximating the quality of the fault location. We use the square root of the LES value and normalize it, not with respect to the highest value for any assumed fault location but with respect to the rms magnitudes of the change-in-fault-location-voltage signals, as follows:

$$\varepsilon = \frac{S_A}{S_B} \cdot 100\% \tag{11}$$

where:

$$S_A = \sqrt{\sum_{\Phi\Phi=AB}^{CA} \sum_{T_W} (\Delta v_{FL\Phi\Phi} - \Delta v_{FR\Phi\Phi})^2} \tag{12}$$

$$S_B = \sqrt{\sum_{\Phi\Phi=AB}^{CA} \sum_{T_W} \Delta v_{FL\Phi\Phi}{}^2} + \sqrt{\sum_{\Phi\Phi=AB}^{CA} \sum_{T_W} \Delta v_{FR\Phi\Phi}{}^2} \tag{13}$$

The goodness of fit value, ε, is a Euclidean distance between the two change-in-fault-location-voltage signals in per unit of the Euclidean norms of these signals. By using this definition, we do not consider all potential fault locations (like in Fig. 6). We consider only the location obtained from our method.

The ε value is always between 0 and 100 percent. ε = 0 if the two signals are identical (perfect fit, maximum similarity). ε = 100 if the two signals are as different as possible (identical in value and opposite in polarity, maximum dissimilarity).

To develop an intuitive understanding of ε, consider that if the local and remote change-in-fault-location-voltage estimates differ on average by 1 percent, the ε value is about 0.5 percent. An elevated ε value can indicate the following issues: CCVT transients that make the shape of the incremental voltages different between the terminals, CT saturation that makes the shape of the incremental replica currents different between the terminals, large capacitive charging current (as compared to the fault current) that makes the method less accurate, and large line-side reactor currents (as compared to the fault current) that similarly make the method less accurate. The ε value may provide a degree of confidence for the accuracy of the fault-locating result, but it cannot be solely relied on as a true accuracy indicator. That is, we generally expect that a low ε value is consistent with an accurate fault-locating result. However, there may be cases where the fault location is highly accurate even though the ε value is high and vice versa. It is good practice to inspect the relay signals if the ε value is greater than about 2 percent.

The ε value for the case shown in Fig. 5 is 1.4 percent and indicates a high quality of the fault-locating result. Of course, the accuracy may be affected by errors in the line impedance setting or the line length setting, but the 1.4 percent value implies that the performance of the method was nearly perfect given the measurements and settings.

## B. *Evolving Fault*

A UHS relay [5] installed on a 161 kV, 72.78 mi line in a 60 Hz system recorded an AG fault that evolved after 11 ms into an ACG fault. Fig. 7 shows the local and remote voltages and currents. The relays were installed in an evaluation mode and did not trip the breakers, hence, the relatively long fault duration.

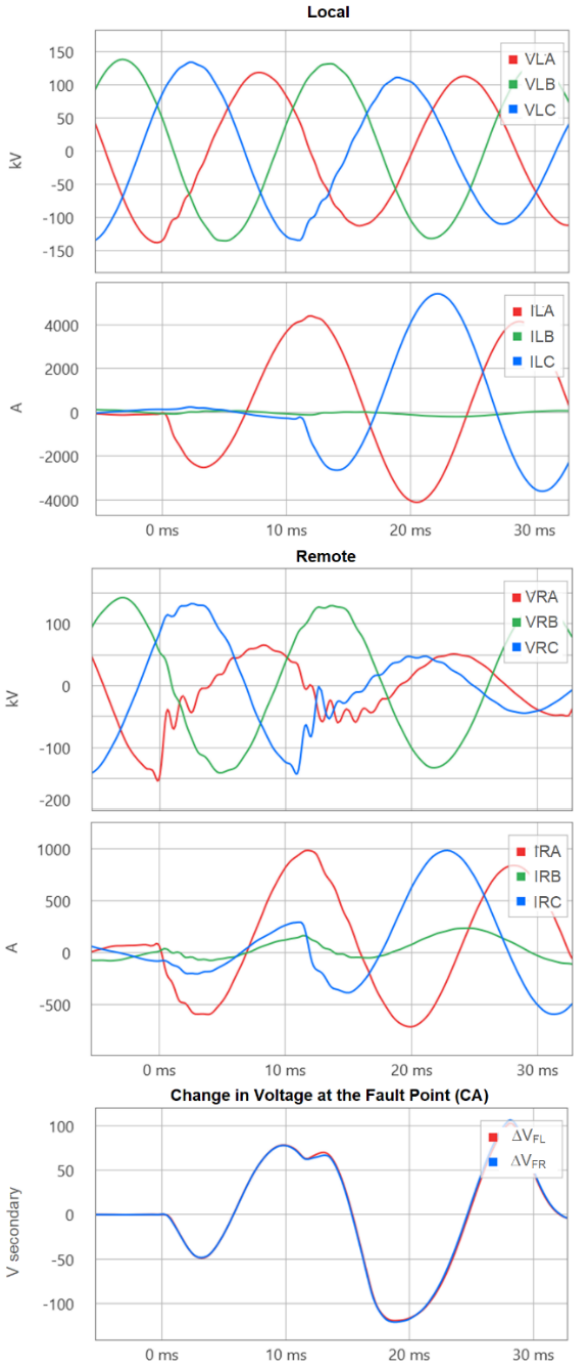


Fig. 7. Evolving fault example.

By using the TW record, we obtained the true fault location of 27.638 mi. Our method calculated 27.706 mi (an error of 0.1 percent of the line length).

Fig. 7 shows the change-in-fault-location-voltage signals (the CA loop) calculated from both terminals of the line

according to the new fault-locating method. The two estimates (the red and blue traces in the bottom plot) match very well, as expected for an accurate fault-locating result. Note that the change-in-fault-location-voltage signals experience a new transient when the second fault occurs 11 ms after the initial fault. As expected, the two signals continue to match after the fault evolves.

A traditional phasor-based fault-locating method would face problems in this case because the phasors do not stabilize during the first fault. The fault evolves in 11 ms or 0.66 cycle. Therefore, the full-cycle phasors would stabilize at 0.66 cycles + 1.25 cycles = 1.91 cycles. If the UHS relay [5] had been wired to trip, the fault would have been cleared by then.

### C. *Incipient Fault*

A UHS relay [6] installed on a 275 kV, 352.58 km line in a 50 Hz system recorded an internal event in the C phase. Fig. 8 shows the local and remote voltages and currents. We are confident that this event was internal to the line because of the following evidence:

- The event direction is forward at both line terminals. The voltage and current shift in opposite directions, indicating a forward event [4].
- The TD32 incremental-quantity directional elements asserted in the forward direction at both line terminals. These elements have a solid security record in the field, and they operated correctly in this case.
- The polarities and arrival times of multiple current TWs at the local and remote terminals are consistent with an internal event occurring 195.83 km from the local terminal, according to the TW fault-locating method.
- The polarities of the first current TWs at the local and remote terminals are consistent with the polarity of the pre-fault voltage at the event location.

We do not have confirmation from the user regarding the location or nature of this event. We know surge arresters are installed along the line and the event could have been the result of an arrester conduction. We are confident, however, that the event happened 195.83 km from the local terminal.

Although the UHS relays [6] were installed in an evaluation mode and did not control the breakers, the POTT scheme operated for this event, giving the user an option to trip for this kind of event. If tripping for this short-lived self-healing event is not desired, the user can desensitize the POTT scheme by increasing the incremental overcurrent pickup threshold [4] [6].

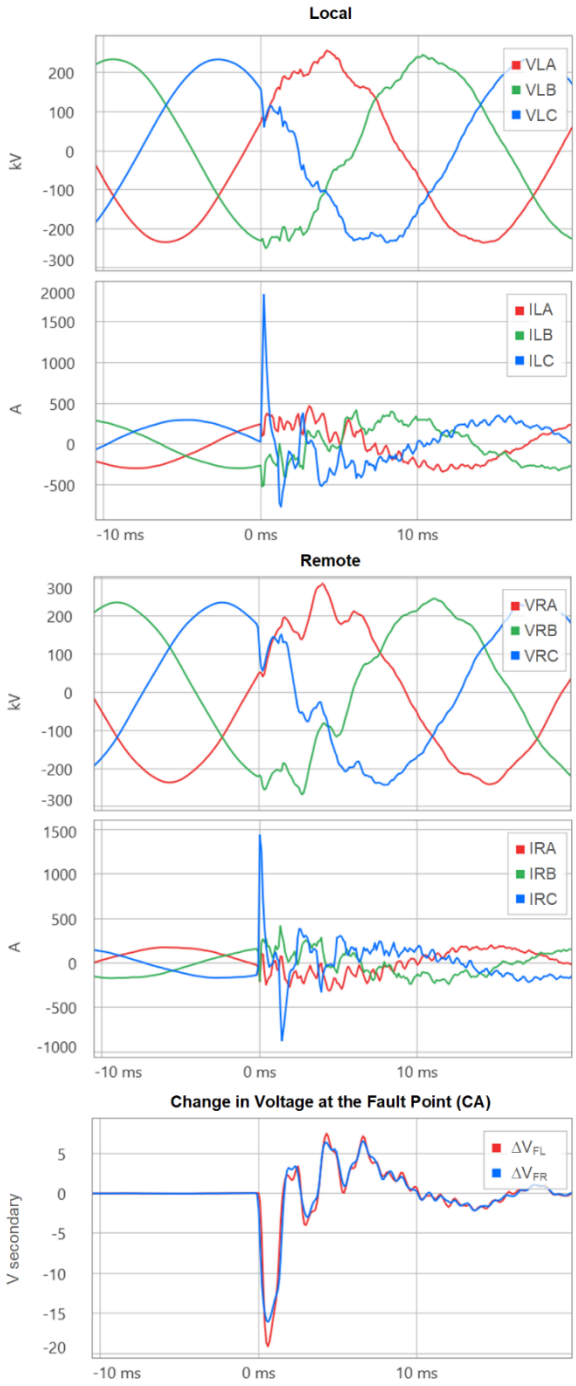


Fig. 8. Incipient fault example.

Our new fault-locating method located this event 185.47 km from the local terminal. Comparing this result to the TW-based location, the error is 2.9 percent of the line length. This result is very encouraging, considering that the elevated current lasted a fraction of a millisecond and the line is very long and had significant charging current oscillating for a long time after the event briefly changed the voltage. Fig. 8 shows the change-in-fault-location-voltage signals (the CA loop) calculated from both terminals of the line according to the new fault-locating method (the red and blue traces in the bottom plot). The change-in-fault-location-voltage signal is relatively small (about 10 percent of nominal voltage) and dominated by an oscillatory

300 Hz component. The change-in-fault-location-voltage signals estimated from the local and remote terminals match reasonably well, but not perfectly. Specifically, the peak values in the local estimate are slightly higher than in the remote estimate, and there are higher frequency oscillatory components on the order of about 1.4 kHz that differ between the two estimates. We attribute these differences to the line charging current. To improve the match, we lower the cut-off frequency in the low-pass filter. We can use (11), (12), and (13) to calculate the goodness of fit value for this case and obtain 14.6 percent. Based on our experience (see Section IX) this value may indicate that the locating error is at the level of several percent of the line length.

Overall, the method performs very well given it is working with transients and no fundamental-frequency signals that encode the event location.

### *D. Arcing High-Resistance Fault*

A UHS relay [6] installed on a 230 kV, 68.99 mi line in a 60 Hz system recorded an arcing high-resistance BG fault. Fig. 9 shows the local and remote voltages and currents. The TW-based fault locator did not report any results for this fault, most likely because of fault precursors and TW activity prior to the rise of the fault current.

Fig. 9 shows the change-in-fault-location-voltage signals (the AB loop) calculated from both terminals of the line according to the new fault-locating method (the red and blue traces in the bottom plot). The change-in-fault-location-voltage signal is small (about 5 percent of nominal voltage) and rich in harmonics. Because the voltage at the fault location does not change much, the fault resistance must be very high. Additionally, the current continues to gradually increase from the load level to the fault level. This pattern suggests that the fault path becomes more conductive with the passing of time, as is the case for an arcing fault, a fault caused by a tree contact, or a fault caused by fire inside the line right of way (such as a sugar cane fire).

The utility reported the true fault location (see Fig. 10) as 24.6 mi. Our method calculated 23.79 mi (an error of 1.1 percent of the line length). The two change-in-fault-location-voltage signals match very well (the red and blue traces in the bottom plot of Fig. 9), as expected for an accurate fault-locating result, despite the fault resistance being high, nonlinear, and decreasing with time.

A traditional phasor-based fault-locating method would face challenges for this fault. The phasors do not stabilize because the voltage and current phasors keep changing, and the high fault resistance adds other challenges. The single-ended impedance-based method reported the fault location as 36.522 mi (an error of 17 percent of the line length). The fault resistance and the nonstationary nature of the current cause this large error.

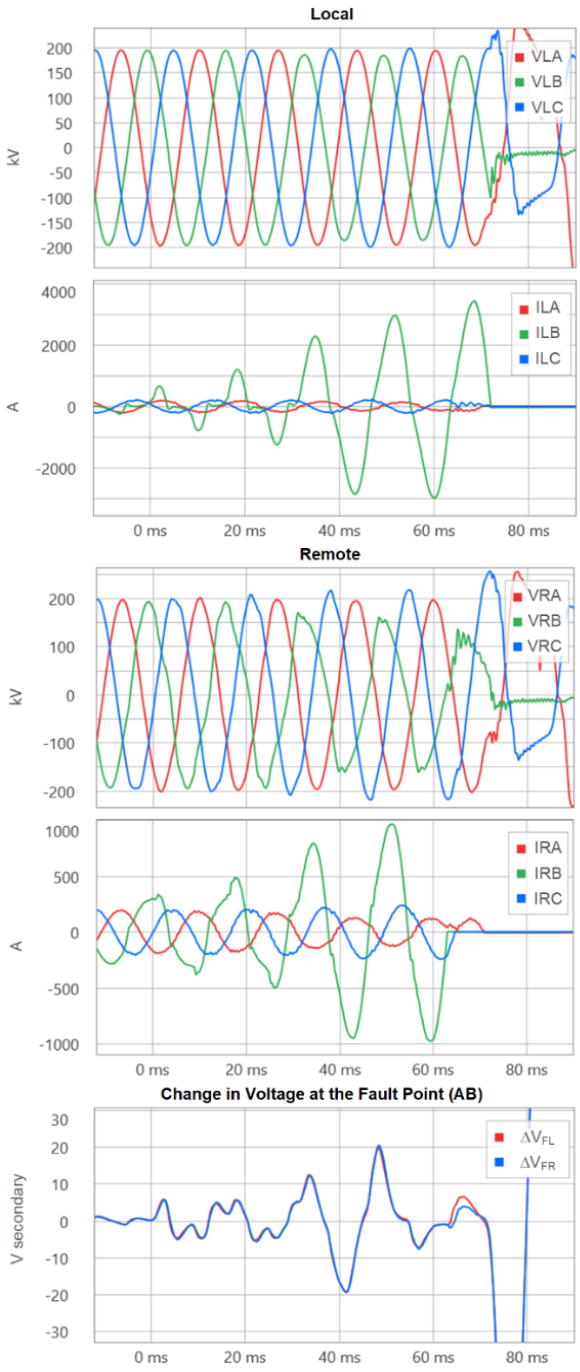


Fig. 9. Arcing high-resistance fault example.

Fig. 10. A tree contact was the cause of the fault shown in Fig. 9 (photograph and fault records courtesy of Puget Sound Energy).

### E. *Fault During a Single-Pole-Open Interval*

A UHS relay [5] installed on a 230 kV, 28.4 km line in a 60 Hz system recorded a fault during a single-pole-open interval. Fig. 11 shows the local and remote voltages and currents. The protection system issued a single-pole trip for the initial CG fault (not shown in the figure). 90 ms after the breakers opened the C pole, a second fault (AG) occurred. Fig. 11 shows the beginning of the second fault. The C-phase voltage is not zero because of the coupling to the energized A and B phases. When the second fault happens, the C-phase voltage changes because of the voltage component induced from the A-phase current.

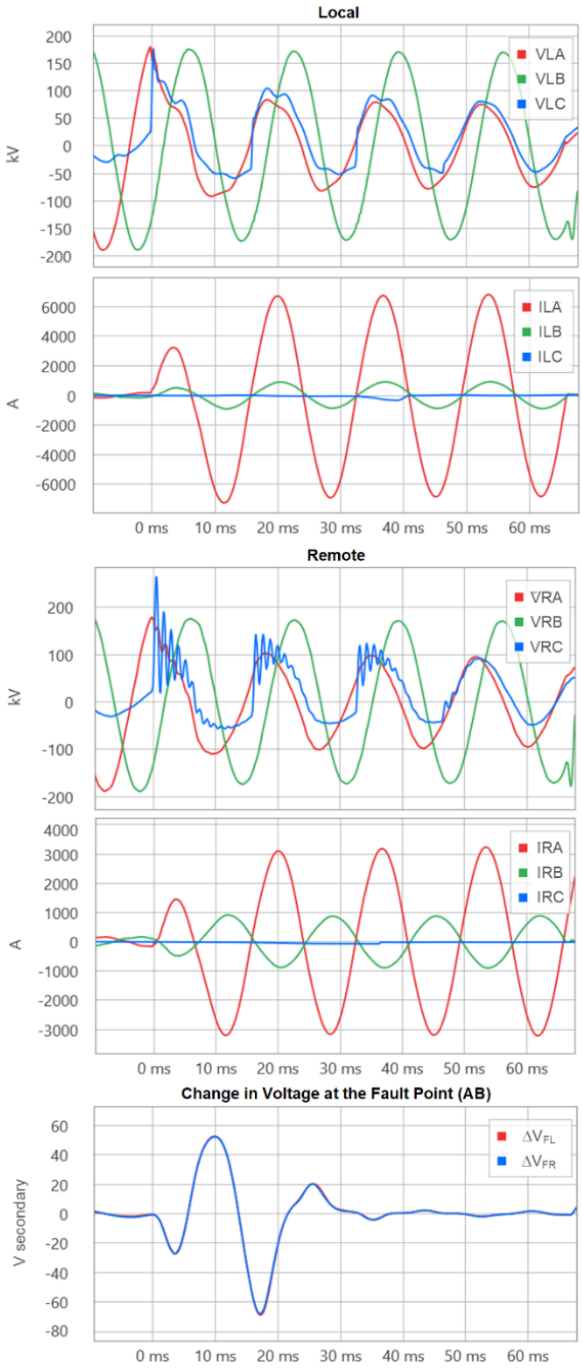


Fig. 11. An AG fault during a C-pole-open interval.

We obtained the true fault location of 3.267 km for the second fault by using the TW record. Our method calculated 3.01 km (an error of 0.9 percent of the line length).

Fig. 11 shows the change-in-fault-location-voltage signals (the AB loop) calculated from both terminals of the line according to the new fault-locating method. The two change-in-fault-location-voltage estimates (the red and blue traces in the bottom plot) match very well, as expected for an accurate fault-locating result, despite the fact that the line operated under the single-pole-open condition. During the C-phase open condition, the method processes only the AB loop to avoid using the C-phase voltage because this voltage is not related to the fault location, especially if the relay is connected to bus-side VTs or the line has line-side reactors installed.

Because of the open-pole condition, single-ended phasor-based fault-locating methods would face challenges because they cannot use any of the typical polarizing signals, such as the negative-sequence current.

## IV. Accuracy Considerations

As the previous section illustrates, the new method is accurate and robust. In this section, we consider several application and accuracy factors. Reference [7] contains more information on fault-locating errors in general.

### A. *Instrument Transformer and Relay Input Errors*

The method is based on voltages and currents, and therefore the instrument transformer and relay input errors affect the fault-locating accuracy. However, because the method is a double-ended method and it uses measurements from three phase-to-phase loops, these errors have a high probability of partially canceling (the method uses 12 signals irrespective of the fault type).

Current transformer (CT) saturation errors and CCVT transient errors are significantly higher than ratio errors, and therefore they impact the fault-locating accuracy to a higher degree. Our method can be enhanced to avoid using fault loops that contain significant CT or CCVT errors. For example, if the A-phase CT saturates during an AB fault, the method can use the BC loop instead of all three loops, and by doing so, it avoids using the A-phase current from a saturated CT.

### B. *Remote Data Alignment Errors*

The method uses the local and remote voltages and currents and requires these two data sets to be time-aligned. A data alignment error may affect the fault-locating accuracy. However, owing to the relative homogeneity of the incremental-quantity equivalent network, especially for the phase loops, one may correct the method for the data misalignment. In homogeneous networks, the change-in-fault-location-voltage signals calculated from the local and remote terminals are in phase, and one may just shift the remote signal to align with the local signal before matching the signal magnitudes by using the LES algorithm (see Fig. 3, Fig. 5, Fig. 7, Fig. 8, Fig. 9, and Fig. 11). Section VIII discusses applications with records that are not time-aligned and ways to

detect and compensate for poor alignment in installations that are expected to provide time-aligned fault records.

### C. Line Characteristics and Mutual Coupling

Line impedance errors affect fault-locating accuracy. Our method avoids using the zero-sequence line impedance for ground faults, and as a result, it has better accuracy (no impact from soil resistivity and mutual coupling). Using all three phase loops for all fault types allows the method to average (at least partially) errors related to line transposition. The voltage-drop equations (2) and (3) neglect the line capacitance, resulting in a small error. Applying low-pass filtering to the change-in-fault-location-voltage signals remediates this issue to a great degree (all examples in this paper apply low-pass filtering). Additionally, the voltage-drop equations (2) and (3) can be expanded to approximate the line charging current in the time domain and further improve the fault-locating accuracy.

We may use fault records for external faults to fine-tune the line impedance magnitude [8]. To apply this concept to our method, we find the value of $|Z_1|$ that minimizes the LES difference between two voltage values: 1) the measured change in voltage at the remote terminal and 2) the change in voltage at the remote terminal calculated from the change in voltage at the local terminal and the line incremental replica current. This process results in (14):

$$|Z_1| = \frac{S_P}{S_Q} \tag{14}$$

where:

$$S_P = \sum_{\Phi\Phi=AB}^{CA} \sum_{T_W} (\Delta v_{L\Phi\Phi} - \Delta v_{R\Phi\Phi}) \cdot (\Delta i_{ZL\Phi\Phi} - \Delta i_{ZR\Phi\Phi}) \tag{15}$$

$$S_Q = \frac{1}{2} \cdot \sum_{\Phi\Phi=AB}^{CA} \sum_{T_W} (\Delta i_{ZL\Phi\Phi} - \Delta i_{ZR\Phi\Phi})^2 \tag{16}$$

In the above equations, we used half of the difference of the local and remote currents for better accuracy (for external faults, the two currents are ideally identical in value and opposite in polarity).

Using external faults to fine-tune the line impedance magnitude can improve the overall experience over the fault locator installation lifespan. However, (14) to (16) yield numerically accurate results only if the incremental voltage drop across the line is sufficiently above the VT and relay voltage measurement errors. Before using the equations to fine-tune the $|Z_1|$ magnitude, ensure that the difference between the local and remote terminals in the incremental phase-to-phase voltages that include the faulted phase(s) is greater than 10 percent of the nominal voltage.

### D. High-Resistance Faults and Arcing Faults

The method works by matching the change-in-fault-location-voltage signals obtained from both ends of the line on a sample-by-sample basis. As such, the method is not concerned with the shape of the change-in-fault-location-voltage signal. As a result, the method works very well for high-resistance faults and for arcing or even intermittent faults. Of course, a fault with extremely high resistance would not depress the voltage at the fault location much, and as a result, the method would operate on signals that are low relative to the measuring range of the VTs and the relays (see Fig. 9). Operating on low voltage signals would increase the fault-locating error. However, in general, the method works substantially better for resistive faults than impedance-based and traveling-wave-based methods (see Subsection III.D).

### E. Evolving Faults

The method works by evaluating all three phase loops, and as such, it does not need to know which phases are involved in the fault. As a result, the method works inherently well, even if the fault evolves within the LES data window (see Subsection III.B).

It is also important to realize that an external unbalance does not upset the voltage-drop equations (2) and (3). Specifically, an external fault could occur immediately before, simultaneously with, or immediately after the internal fault, and the method will perform well despite the external fault. Similarly, if a switching event occurs immediately before, simultaneously with, or immediately after the internal fault, the voltage-drop equations (2) and (3) hold, and the method works well.

Two simultaneous or nearly simultaneous internal faults at different locations is another special case to consider. Such faults could happen as a result of back flashover during lightning strikes or because of the voltage swell in the healthy phases as a result of the initial single-phase-to-ground fault. Our method can be used to detect the presence of two internal faults. When applied to loops that involve faulted phases, the method yields similar results in each loop as long as there is only one fault in a particular location. If different loops yield different results, it is likely that the line has two or more simultaneous faults at different locations. Calculating the fault location separately for all six loops may allow us to locate both faults.

### F. Faults During Single-Pole-Open Conditions

In single-pole tripping and reclosing applications, the line may suffer a second fault during the single-pole-open interval. Traditional impedance-based fault locators face challenges in locating such faults because the open-pole condition prevents the application of advanced polarizing methods, such as using the negative-sequence current. Our method performs very well because the voltage-drop equations (2) and (3) hold even if some breaker poles are opened. However, because the line-side voltage in the open phase is coupled to the energized phases and may exhibit ringing if line-side reactors are installed, apply our method only on the phase loop that does not involve the open phase. For example, if the C pole is opened, the method suppresses the BC and CA loops in the sums (9) and (10), and by doing so, it uses only the AB loop. All fault types that may happen during the C-pole-open condition (AG, BG, AB, and ABG) change the AB voltage and allow the method to operate correctly (see Subsection III.E).

### G. Incipient Cable Faults

The method can locate incipient cable faults. Because often the cable protection system does not trip for these faults (they self-extinguish before the protection elements or schemes can operate), use a disturbance detector to trigger the fault locator to perform the calculations. When our method is triggered unintentionally for an external event, such as by a switching event or an external fault, our method yields a meaningless fault location. You can dismiss these invalid results based on the fault location values and by comparing polarities of the local and remote incremental replica currents and rejecting cases for which the polarities do not match. See Section VI for more information on applications to cable lines.

### H. Line Terminations, Fault Distance, and Point on Wave

TW-based methods have a proven track record in the field of locating faults to within a tower span (300 m or 1,000 ft), and they have good dependability for a wide range of faults and system conditions. However, these methods do have dependability challenges, including application to short lines and – when using currents only – lines terminated with a high surge impedance, such as with only a power transformer or series reactor. Furthermore, faults that occur close to a line terminal or a tap or near a voltage zero-crossing may also challenge the dependability of TW-based methods. The method described in this paper is not affected by line terminations, line length, line taps, fault distance, or fault point on wave. Therefore, it remains highly dependable and accurate under these conditions.

A special termination case is a line-end-open condition. A double-ended TW-based fault-locating method that is based on current would fail in this case. Of course, the single-ended impedance-based method would work reasonably well because there is no infeed effect from the open line terminal. Our method works well as long as the voltage is measured on the line side of the open breaker as is typically the case in high-voltage applications (Fig. 12). As we would expect, the voltage rise along the line due to the line capacitance (the Ferranti effect, not shown in Fig. 12) may degrade the accuracy of fault locating to some degree.

Naturally, the method works well if one of the terminals is very weak (very small change in current and voltage as opposed to no change in current as shown in Fig. 12). Note, however, that faults always cause some change in either voltage or current, even if the terminal connects only loads and not sources.

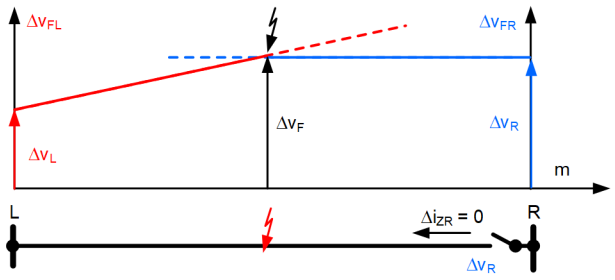


Fig. 12. Illustration of the method operation during a line-end-open condition.

## V. Application to Multiterminal Lines

You can apply the new method to multiterminal lines (lines with three or more terminals) by following this three-step procedure:

1. Identify the faulted section by matching the change-in-voltage signals at the line tap location(s).
2. Calculate the incremental voltages and incremental replica currents at the terminals of the faulted section.
3. Apply the two-terminal method from Section II to the faulted line section.

Consider the three-terminal line shown in Fig. 13.

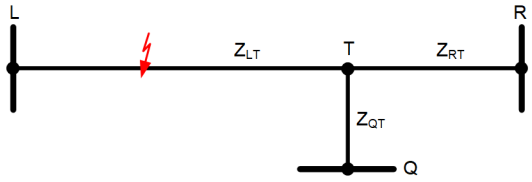


Fig. 13. Three-terminal line example.

The method calculates the change-in-voltage-at-the-tap (T) signals, assuming all line sections are healthy:

$$\Delta v_{TL} = \Delta v_L - |Z_{LT}| \cdot \Delta i_{ZL} \quad (17)$$

$$\Delta v_{TR} = \Delta v_R - |Z_{RT}| \cdot \Delta i_{ZR} \quad (18)$$

$$\Delta v_{TQ} = \Delta v_Q - |Z_{QT}| \cdot \Delta i_{ZQ} \quad (19)$$

For the case shown in Fig. 13, (18) and (19) yield very similar values but (17) yields a different value because the fault makes (17) inaccurate. These results confirm that section LT is faulted and sections RT and QT are healthy. To compare the change-in-voltage-at-the-tap signals, use the squared differences between (17), (18), and (19) over the same data window as in the fault-locating calculations. For example, to compare (17) and (18), use:

$$\sum_{\Phi\Phi=AB}^{CA} \sum_{TW} (\Delta v_{TL\Phi\Phi} - \Delta v_{TR\Phi\Phi})^2 \quad (20)$$

Knowing that the LT section is faulted, the method calculates the incremental voltage and incremental replica current at the tap T of the faulted section as follows:

$$\Delta v_T = \frac{1}{2}\left(\Delta v_{TR} + \Delta v_{TQ}\right) \quad (21)$$

$$\Delta i_{ZT} = \Delta i_{ZR} + \Delta i_{ZQ} \quad (22)$$

Equation (21) averages the two voltage calculations from the R and Q terminals to provide additional accuracy (the two values being averaged are ideally the same). Equation (22) follows Kirchhoff's current law for the node T.

Finally, the method applies the two-terminal procedure from Section II to the signals labeled L and T while using the $Z_{LT}$ line section impedance. The fault-locating result is in per unit of the faulted line section LT.

When the line sections are not homogeneous (i.e., they have different X/R ratios), obtain the replica currents (1) and use the corresponding line section impedance: $Z_{LT}$ in (17), $Z_{RT}$ in (18), $Z_{QT}$ in (19), and $Z_{LT}$ in (22).

## VI. Application to Cable Lines

Underground or undersea cables differ from overhead lines in many respects. On the basis of per unit of length, they have lower impedance but draw higher capacitive charging current. In single-core cables, all conductors are shielded as a group. In three-core cables, each phase conductor is shielded separately. The shields may be bonded and grounded along the cable path. As a result, the zero-sequence representation of a cable may differ from that of an overhead line. Phase faults in single-core cables are practically impossible, and most faults are ground faults. Phase-to-phase mutual impedances in single-core cables are practically zero. Given all these characteristics, can we apply our approach of using phase-to-phase loops to fault locating in cables?

To answer the question, it is important to realize that the differences between cables and overhead lines are of degree and not kind. An overhead line operates with ground under the conductors and in the presence of a shield wire that may also be grounded along the line path. As a result, we can represent both a cable and an overhead line by using the same line impedance matrix, except the matrix for a cable has significantly different values than the matrix for an overhead line. Owing to this mathematical similarity, we can state that our method of using phase-to-phase loops to locate ground faults in cables works correctly.

Moreover, by avoiding the zero-sequence line impedance and voltage and current components, the method has better accuracy than traditional fault-locating methods that work with ground loops. Consider the following field case as an example.

A line current differential relay [3] installed on a 345 kV, 9.40 mi underground cable in a 60 Hz system tripped for a BG fault. Fig. 14 shows the local and remote voltages and currents.

The utility reported that the fault was a failed arrester within the cable protection zone at the remote substation. We substantiate this information in Fig. 15 by plotting the faulted-phase differential current to approximate the fault path current. The current waveform shows a pattern consistent with repeated starting and stopping of a current flow with the periods of no conduction getting progressively shorter and the magnitude increasing until the point of total failure and the rise of the large fault current at t = 0, as shown in Fig. 14 and Fig. 15.

Our method calculated a fault location of 9.121 mi (i.e., 0.279 mi away from the remote substation). Fig. 14 shows the BC change-in-fault-location-voltage signals calculated from the local and remote terminals. These signals match very well, indicating a high confidence level for the accuracy of the fault-locating result. The fault location error of 0.279 mi (1,470 ft, 450 m, or 3 percent of the line length) is likely a combination of instrument transformer errors, finite line impedance accuracy, and the cable charging current. Additionally, the VT and the busbar may be some distance apart from the location of the arrester at the overhead-cable junction. In other words, there is a possibility that the failed arrester was located not at the remote VT but some distance away from it.

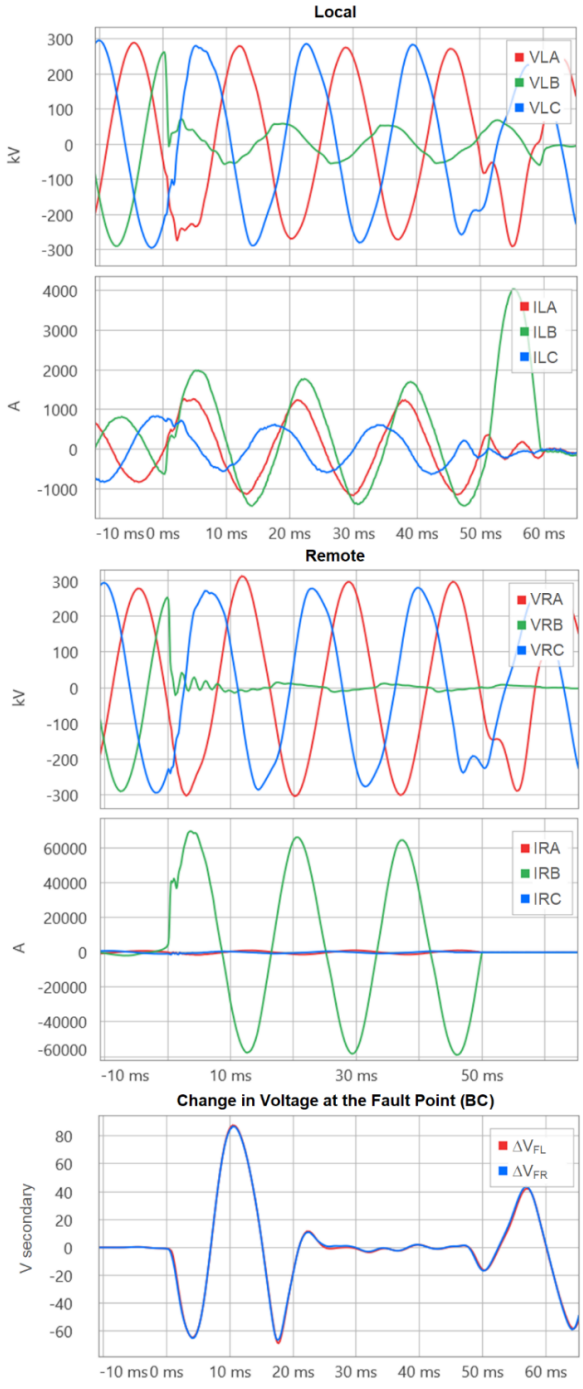


Fig. 14. Cable fault example.

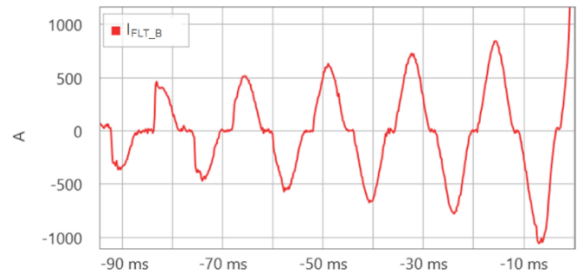


Fig. 15. Differential B-phase current.

## VII. Application to Hybrid Lines

We can apply the new method to hybrid lines comprising overhead line (OHL) sections and underground cable (UGC) sections by following this multistep procedure:

1. Assume a faulted section of the line.
2. Calculate the incremental voltages at both terminals of the faulted line section by using the local and remote voltages and currents.
3. Apply the two-terminal method from Section II to the faulted line section.
4. Determine if the calculated fault location falls within the line section that you assumed to be faulted. If it does, you have obtained the true fault location. If it does not, return to step 1 of this procedure and assume a different faulted section, progressing along all line sections.

Consider the hybrid line with two overhead line sections and one underground cable section shown in Fig. 16.

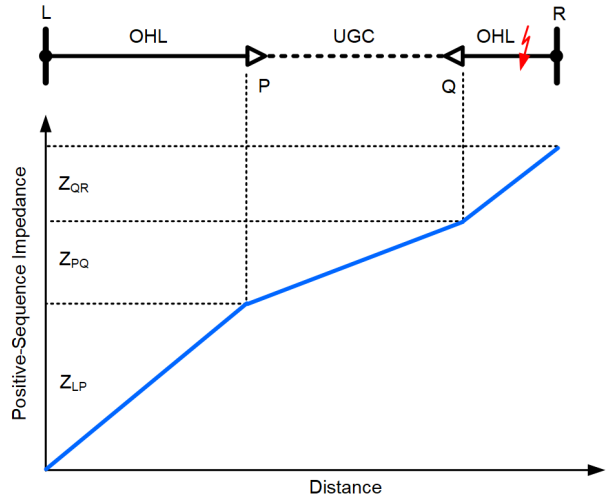


Fig. 16. Hybrid line example.

Because hybrid lines are nonhomogeneous, we cannot use the replica incremental currents derived from the measured local and remote currents to calculate the incremental voltages along the line segments. Instead, when calculating the incremental voltages, we must account for the impedance between the relay location and the point of interest. Similarly, when calculating the replica incremental currents, we must use the impedance of the assumed faulted section. Consider the following example.

We assume the fault is located on the LP section of the line shown in Fig. 16. The change in voltage at the L terminal $\Delta v_L$ is a measured value. We calculate the change in voltage at the P junction from the remote voltage and current measurements as follows:

$$\Delta v_{PR} = \Delta v_R - \cdots$$

$$\left( \left(R_{QR} + R_{PQ}\right) \cdot \Delta i_R + \left(L_{QR} + L_{PQ}\right) \cdot \frac{d}{dt} \Delta i_R \right) \qquad (23)$$

We apply the two-terminal method from Section II by using the $\Delta v_L$ voltage, the $\Delta v_{PR}$ voltage (23), and the $\Delta i_L$ and $\Delta i_R$ currents (when calculating the incremental replica currents in step 3, we use the $Z_{LP}$ impedance), and calculate the fault location $m_0$ in per unit of the LP section length. For the case shown in Fig. 16, the calculated $m_0$ is greater than 1 pu, indicating that the fault is not on the LP section of the line.

Knowing the fault is not on the LP section, we assume the fault is on the PQ section of the line and calculate the change in voltage at the P and Q junctions from the local and remote voltage and current measurements as follows:

$$\Delta v_{PL} = \Delta v_L - \left( R_{LP} \cdot \Delta i_L + L_{LP} \cdot \frac{d}{dt} \Delta i_L \right) \qquad (24)$$

$$\Delta v_{QR} = \Delta v_R - \left( R_{RQ} \cdot \Delta i_R + L_{RQ} \cdot \frac{d}{dt} \Delta i_R \right) \qquad (25)$$

We apply the two-terminal method from Section II by using the $\Delta v_{PL}$ voltage (24), the $\Delta v_{QR}$ voltage (25), and the $\Delta i_L$ and $\Delta i_R$ currents (when calculating the incremental replica currents in step 3, we use the $Z_{PQ}$ impedance), and calculate the fault location $m_0$ in per unit of the PQ section length. For the case shown in Fig. 16, the calculated $m_0$ is greater than 1 pu, indicating that the fault is not on the PQ section of the line.

Finally, we assume that the fault is located on the QR section of the line. The change in voltage at the R terminal $\Delta v_R$ is a measured value. We calculate the change in voltage at the Q junction from the local voltage and current measurements as follows:

$$\Delta v_{QL} = \Delta v_L - \cdots$$

$$\left( \left(R_{LP} + R_{PQ}\right) \cdot \Delta i_L + \left(L_{LP} + L_{PQ}\right) \cdot \frac{d}{dt} \Delta i_L \right) \qquad (26)$$

We apply the two-terminal method from Section II by using the $\Delta v_R$ voltage, the $\Delta v_{QL}$ voltage (26), and the $\Delta i_L$ and $\Delta i_R$ currents (when calculating the incremental replica currents in step 3, we use the $Z_{QR}$ impedance), and calculate the fault location $m_0$ in per unit of the QR section length. For the case shown in Fig. 16, the calculated $m_0$ is between 0 pu and 1 pu, indicating that the fault is on the QR section of the line. Fig. 17 illustrates the voltage change profile for the true fault location.

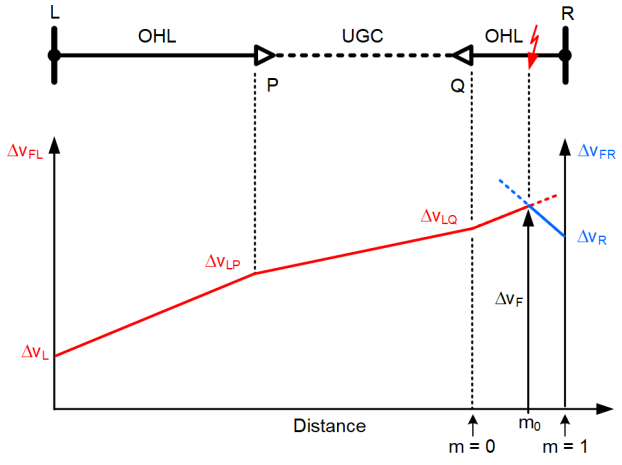


Fig. 17. Voltage change profile for the hybrid line example.

## VIII. Using Records That Are Not Time-Aligned

We can use our method with local and remote records that are not time-aligned. The fault acts as a synchronizing event because the incremental signals rise from zero in the pre-fault state to non-zero values at the fault inception.

We recommend using disturbance-detection logic to obtain a coarse alignment of the local and remote records. Subsequently, we repeat the LES calculations multiple times, shifting the remote data set by as much as ±1 or ±2 ms in steps of one sample to obtain the minimum possible LES value (8).

Fig. 18 illustrates this process for the case from Subsection III.A. The original records are time-aligned but we shift the remote record on purpose to model the lack of alignment. We calculate the fault location and the normalized square root of the LES value – similar to Fig. 6 – for each time shift (see Fig. 18). Notice that when the time shift is restricted to be only in increments of the sampling period (0.1 ms in this case), the minimum LES value occurs when the time shift is 0 ms. However, we can use interpolation when searching for the minimum LES value to improve the data alignment and reach a time resolution better than one sampling period. To perform interpolation, we fit a parabola or a tent shape to the LES value as a function of the time shift (the blue trace shown in Fig. 18) and find the minimum of the fitted shape. The minimum LES value is determined from the intersection point of the two best fit straight lines that use data points on the left and right of the minimum, respectively (dashed blue traces shown in Fig. 18). Finally, we use that interpolated time shift in fractional samples to interpolate the fault location (the red trace shown in Fig. 18). Reference [2] provides more details on using interpolation for improving spatial resolution and accuracy.

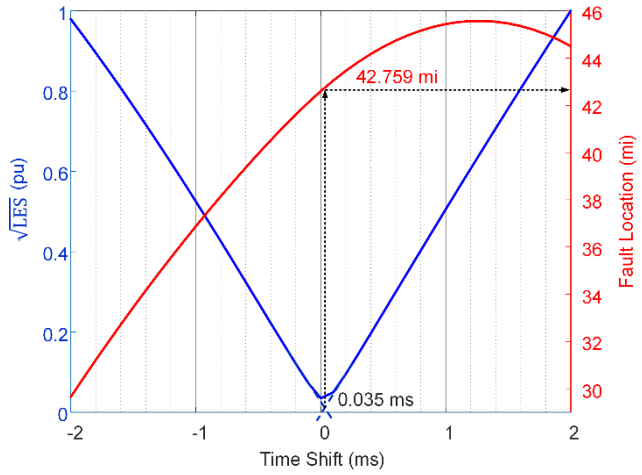


Fig. 18. Sample relationship between the time shift, LES value, and fault location.

The LES value is at its minimum for a time shift of 0.035 ms. The original record comes from a scheme with the worst-case time alignment accuracy of 200 ns [5] and typical accuracy of 50 ns. The 200 ns worst-case timing error is negligible compared with the 0.035 ms time shift. Therefore, we can assume that the original alignment is perfect and claim that our method can align records with an accuracy of about 35 μs when working with samples captured at a rate of 10 ksps.

Our alignment method is robust because manipulating the m value for a time-shifted record cannot accurately match the change in voltage at the fault location calculated from the local and remote terminals. Instead, the best fit can only be obtained by correctly time-shifting the records before manipulating the m value. As a result, we can be confident that the time shift that minimizes the LES value is the shift that correctly aligns the local and remote records.

The presented alignment method allows us to locate faults by using records that are not time-aligned. In the example of Fig. 18, the fault location that corresponds to the minimum LES value at 0.035 ms is 42.759 mi (we interpolate the m value). Fault locating performed on the aligned data yielded 42.603 mi, and the utility-confirmed location was 41.91 mi (see Subsection III.A). To summarize, using records that were not time-aligned introduced an error of only 0.156 mi (823 ft or 251 m).

The fault-locating method that seeks to minimize the LES value by considering both the fault location and the time-shift as variables allows us to detect and compensate for poor alignment in installations that are expected to provide time-aligned fault records.

In general, we can always execute our fault-locating method by assuming both the fault location and the time-shift as variables. This approach may be beneficial for very long lines with long TW propagation times. For faults on long lines, the TWs that are the first indicators of the disturbance may arrive at the opposite line terminals at times as different as 1 ms, creating an impression of data misalignment. Treating the time-shift as a variable in these cases allows us to bridge the gap between the actual line with finite and significant TW propagation times and the lumped-parameter line model that we used to derive the fault-locating method.

## IX. Accuracy Tested on Field Cases

We have tested the new method by using 118 fault records that the UHS line protective relays [5] and [6] captured in the field for internal faults on two-terminal overhead lines. To allow for fast tripping, these relays derive and low-pass filter the incremental voltages and incremental replica currents. The relays include these signals in their IEEE COMTRADE records. We have used these 10 ksps records to test our fault-locating method offline. Because the input signals already reflect all practical error sources (instrument transformers, relay inputs, data alignment, fault resistance, line impedance, line transposition, line charging current, and so on), these test results are highly relevant and informative. To calculate the fault-locating error, we used the utility-confirmed (“true”) fault location. If we did not have a confirmed fault location from the utility, we used the TW-based fault-locating results after carefully reviewing and fine-tuning them.

Table I shows a sample set of 25 cases. Our fault-locating method is very dependable and accurate (1.1 percent average error). The outliers, such as the case of 6.9 percent maximum error, are caused by CCVT transients (including cases where bushing potential devices were used) or CT saturation.

TABLE I
FIELD CASES AND TEST RESULTS

| Case | Voltage (kV) | Length (km) | Fault Type | Location (km) | | Error (%) |
|---|---|---|---|---|---|---|
| | | | | True | Calc. | |
| 1 | 115 | 92.7 | AG | 53.7 | 53.5 | 0.2 |
| 2 | 115 | 93.0 | BG | 61.0 | 60.7 | 0.2 |
| 3 | 115 | 138.5 | ABG | 108.0 | 107.4 | 0.4 |
| 4 | 132 | 59.0 | AB | 32.6 | 33.3 | 1.1 |
| 5 | 138 | 38.2 | CG | 17.2 | 17.3 | 0.3 |
| 6 | 138 | 74.2 | CG | 23.8 | 23.9 | 0.2 |
| 7 | 144 | 99.8 | AB | 63.5 | 60.7 | 2.8 |
| 8 | 154 | 39.7 | ABC | 19.7 | 19.2 | 1.3 |
| 9 | 161 | 117.1 | CAG | 44.5 | 43.6 | 0.8 |
| 10 | 220 | 27.5 | AB | 21.0 | 20.8 | 0.8 |
| 11 | 220 | 62.0 | BG | 33.9 | 34.1 | 0.4 |
| 12 | 220 | 73.8 | AG | 31.8 | 32.0 | 0.3 |
| 13 | 220 | 113.6 | CG | 92.3 | 94.0 | 1.4 |
| 14 | 230 | 28.4 | CG | 3.3 | 3.3 | 0.0 |
| 15 | 230 | 28.5 | CG | 17.5 | 17.5 | 0.1 |
| 16 | 230 | 40.6 | AG | 38.4 | 38.8 | 1.0 |
| 17 | 230 | 50.5 | CG | 43.4 | 42.9 | 1.0 |
| 18 | 230 | 153.2 | CG | 61.5 | 60.4 | 0.7 |
| 19 | 275 | 352.6 | CG | 244.0 | 239.5 | 1.3 |
| 20 | 345 | 55.2 | AG | 17.0 | 15.9 | 2.0 |
| 21 | 345 | 64.2 | CG | 37.8 | 37.7 | 0.2 |
| 22 | 345 | 75.8 | AG | 73.5 | 73.1 | 0.5 |
| 23 | 345 | 113.3 | CG | 50.5 | 50.4 | 0.1 |
| 24 | 345 | 113.3 | AG | 105.7 | 105.7 | 0.1 |
| 25 | 345 | 190.9 | BG | 97.9 | 98.3 | 0.2 |
| Average error (all 118 cases) | | | | | | 1.1 |
| Maximum error (all 118 cases) | | | | | | 6.9 |

## X. CONCLUSIONS

This paper presents a new multi-ended fault-locating method that works in the time domain. Our primary motivation was to develop a method that works in conjunction with the UHS relays, because these relays may limit the total fault duration to 1.5 cycles and prevent the full-cycle phasor estimators from obtaining stable measurements.

The new method has several other benefits. It works well for incipient, intermittent, high-resistance, arcing and evolving faults (including simultaneous internal and external faults), and faults during single-pole-open conditions. The method does not need faulted-loop selection logic, and it does not use the zero-sequence line impedance, avoiding errors associated with that impedance and errors related to the zero-sequence voltage and current components in general. The method can be applied to multiterminal, cable, and hybrid lines and can use remote fault records that are not aligned with local records.

We have tested the new method on a large set of field records and proved exceptional dependability and very good accuracy.

The paper includes many application considerations and techniques to improve accuracy of fault locating and line impedance data.

## XI. REFERENCES


[1] B. Kasztenny and G. Smelich, "Using incremental quantities to locate faults: a new double-ended method for ultra-high-speed protective relays," proceedings of the 19th IET Conference on Developments in Power System Protection, Bilbao, Spain, 2025, pp. 6-13, doi: 10.1049/icp.2025.1039.

[2] E. O. Schweitzer, III, A. Guzmán, M. V. Mynam, V. Skendzic, B. Kasztenny, and S. Marx, "Locating Faults by the Traveling Waves They Launch," proceedings of the 40th Annual Western Protective Relay Conference, Spokane, WA, October 2013.

[3] *SEL-411L Instruction Manual*. Available: selinc.com.

[4] E. O. Schweitzer, III, B. Kasztenny, A. Guzmán, V. Skendzic, and M. V. Mynam, "Speed of Line Protection – Can We Break Free of Phasor Limitations?" proceedings of the 41st Annual Western Protective Relay Conference, Spokane, WA, October 2014.

[5] *SEL-T400L Instruction Manual*. Available: selinc.com.

[6] *SEL-T401L Instruction Manual*. Available: selinc.com.

[7] M. M. Saha, J. Izykowski, and E. Rosolowski, *Fault Location on Power Networks*, Springer, 2010.

[8] A. Amberg, A. Rangel, and G. Smelich, "Validating Transmission Line Impedances Using Known Event Data," proceedings of the 65th Annual Conference for Protective Relay Engineers, College Station, TX, April 2012.


## XII. BIOGRAPHIES

**Bogdan Kasztenny** has 35 years of experience in power system protection and control. In his decade-long academic career (1989–1999), Dr. Kasztenny taught power system and digital signal processing courses at several universities and conducted applied research for several relay manufacturers. In 1999, Bogdan left academia for relay manufacturers where he has since designed, applied, and supported protection, control, and fault-locating products with their global installations numbering in the thousands. Bogdan is an IEEE Fellow, an IET Fellow, a Senior Fulbright Fellow, a Distinguished CIGRE Member, and a registered professional engineer in the province of Ontario. Bogdan has served as a Canadian representative of the CIGRE Study Committee B5 (2013–2020) and on the Western Protective Relay Conference Program Committee (2011–2020). In 2019, Bogdan received the IEEE Canada P. D. Ziogas Electric Power Award. Bogdan earned both the Ph.D. (1992) and D.Sc. (Dr. habil., 2019) degrees, has authored over 250 technical papers, and holds over 60 U.S. patents.

**Greg Smelich** earned a BS in mathematical science and an MS in electrical engineering in 2008 and 2011, respectively, from Montana Tech of the University of Montana. Greg then began his career at Schweitzer Engineering Laboratories, Inc. (SEL) as a protection application engineer in the Sales and Customer Service division. In 2016, he transitioned to the Research and Development division as a product engineer, where he now helps guide product development and provides training and technical support primarily related to time-domain technology. He has coauthored several technical papers and application guides on various topics related to power system protection and fault locating. He has been a certified SEL University instructor since 2011 and an adjunct professor in the electrical engineering department at Montana Tech since 2017. Greg is a Senior Member of IEEE and a registered professional engineer in the state of Washington.


20250904 • TP7224-01